BGK electron solitary waves in 3D magnetized plasma

Li-Jen Chen[1,2] and George K. Parks[2,3]

Received 4 May 2001; revised 6 November 2001; accepted 12 November 2001; published 11 May 2002.

[1] This paper presents analytical solutions that we obtained in extending the BGK electron solitary wave solutions in 1D to include the 3D electrical interaction ($E \sim 1/r^2$) of charged particles. Our results indicate that for a single humped electric potential, the parallel cut of the perpendicular component of the electric field ($E_\perp$) is unipolar and that of the parallel component ($E_\parallel$) bipolar. The multi-dimensional features of solitary waves have been observed by the FAST satellite. The parallel width-amplitude relation is found to be an inequality and it depends on the perpendicular scale size of the solitary structure. This feature can be used in conjunction with experimental data to obtain an estimate on the typical perpendicular size of observed solitary waves. *INDEX TERMS:* 7815 Space Plasma Physics: Electrostatic structures; 7839 Space Plasma Physics: Nonlinear phenomena; 7867 Space Plasma Physics: Wave/particle interactions; 2411 Ionosphere: Electric fields (2712)

1. Introduction

[2] The ubiquitous nature of electrostatic solitary waves in the Earth's magnetosphere has recently been revealed by satellite observations from the plasma sheet boundary [*Matsumoto et al.*, 1994; *Cattell et al.*, 1999; *Franz et al.*, 1998], auroral ionosphere [*Temerin et al.*, 1982; *Boström*, 1988; *Mozer et al.*, 1997; *Ergun et al.*, 1998a, 1998b, 1999], bow shock [*Bale et al.*, 1998] and magnetosheath [*Kojima et al.*, 1997]. Solitary waves with either positive or negative potentials have been observed. Negative potential pulses in the auroral upward current region possess features that are unique to Bernstein-Greene-Kruskal (BGK) ion mode solitary waves [*Mälkki et al.*, 1989]. Based on the characteristics of the propagation velocity of solitary waves, the parallel width-amplitude relation, and the associated particle distributions, positive potential pulses observed in the auroral downward current region have been shown to behave like BGK electron solitary waves [*Muschietti et al.*, 1999], also called phase space electron holes (EH). These positive potential pulses detected by the FAST satellite are multi-dimensional with bipolar $E_\parallel$ and unipolar $E_\perp$ [*Ergun et al.*, 1999]. The nonzero $E_\perp$ dictates that the perpendicular span of the solitary wave is finite and a BGK solution based on the 3D Poisson equation is needed.

[3] FAST spacecraft observations have shown that electrons associated with solitary waves are highly field-aligned with a gyroradius $\leq$1 m. This is much less than the typical scale sizes of the solitary waves and the Debye length λ_D that are typically $\sim$100 m. A reasonably good approximation in such a case is to assume that electrons move only along the magnetic field (**B**) direction.

[4] In this paper, we construct a set of analytical BGK solitary wave solutions by solving the coupled 3D Poisson and 1D Vlasov equations. We require the solutions to preserve features of 1D BGK EH solutions in the parallel direction. Additional new information about the nature of the 3D solitary waves will be deduced from the analytical expressions. The structures of the constructed solitary potentials will be examined and a qualitative comparison with FAST observations will be made.

2. The Analytical Model

[5] Our formulation assumes azimuthal symmetry, and that electron motion is along **B** and ions form the uniform background. The first assumption is a natural starting point for a system with a magnetic field. The second is justified since the electron gyroradius ($\leq$1 m) is much less than all relevant scale lengths as discussed in the Introduction. The third assumption is justified because the velocity perturbation of ions due to the self-consistent interaction with the solitary potential is much smaller than that of electrons owing to the large mass ratio, and that the solitary waves move with large velocities ($\sim$1000 km/s) in the ion frame [*Ergun et al.*, 1999]. Therefore, to a good approximation, the ion density can be assumed uniform.

[6] We choose the cylindrical coordinate (r, θ, z) to be the coordinate system, the center of the solitary wave to be the origin, and the unit vector $\hat{z}$ to be along **B**. The dimensionless 3D Poisson equation written in such coordinate system with an azimuthally symmetric potential is

$$\left[\frac{\partial^2}{\partial r^2} + \frac{\partial}{r\partial r} + \frac{\partial^2}{\partial z^2}\right]\Phi(r,z) = -\rho(r,z), \tag{1}$$

where Φ is the electrostatic potential normalized by T_e/e (T_e is the parallel ambient electron thermal energy), ρ the normalized charge density (lengths are normalized by the parallel Debye length λ_D). We search for solutions which give a single humped potential. It is required that the properties of 1D BGK EH solutions to be preserved in the parallel direction. In a 1D BGK EH, the core charge density is positive and the screening (the excess negative charge at the flank) is achieved by electrons trapped and oscillating inside the potential [*Chen and Parks*, 2001]. To sustain such a solitary structure, the core charge density cannot change sign in the perpendicular direction. Therefore, the potential must also have no node in the radial direction. In general, the potential and the charge density can be expanded using the eigenfunctions of the radial differential operator as a complete set of basis. Since the potential is single humped and has no node, the dominant term in the expansion would be J_0 up to its first root. The solitary potential constructed according to the above considerations yields,

$$\Phi(r,z) = \phi_\parallel(z) J_0\left(l_{00}\frac{r}{r_s}\right), \tag{2}$$

where $l_{00} \simeq 2.404$ is the first root of Bessel function J_0, r_s is the perpendicular scale size at which Φ falls to zero, and $\phi_\parallel(z) = \Psi \exp(-z^2/2\delta^2)$ as observations of the parallel profile of the solitary potential fit reasonably a Gaussian [*Ergun et al.*, 1998b].

[7] We use the potential given by Equation (2) and follow the BGK approach [*Bernstein et al.*, 1957] to obtain the trapped electron distribution to demonstrate that the plasma can kinetically

[1]Physics Department, University of Washington, Seattle, WA, USA.
[2]Geophysics Program, University of Washington, Seattle, WA, USA.
[3]Space Science Laboratory, University of California, Berkeley, CA, USA.

0094-8276/02/2001GL013385$05.00

support such a potential. With the assumption that electrons only move along **B**, the Vlasov equation in normalized units becomes

$$v\frac{\partial F(r,z,v)}{\partial z}+\frac{1}{2}\frac{\partial \phi(r,z)}{\partial z}\frac{\partial F(r,z,v)}{\partial v}=0, \tag{3}$$

where F is the electron distribution function, v is the velocity along $\hat{z}$ and is normalized by $v_{te}=\sqrt{2T_e/m_e}$. It is a direct consequence of azimuthal symmetry that there is not only no θ dependence in Φ and F, but also no dependence on perpendicular velocities (V_r and V_θ) in F. The nonzero $E_\perp$ causes only the $\mathbf{E}\times\mathbf{B}$ drift in $-\hat{\theta}$, and no radial velocity. Hence, there will not be any additional terms in Equation (3) even if the $\mathbf{E}\times\mathbf{B}$ drift is included. At a constant radial distance r from the center of the solitary wave, $|E_\perp|$ is constant over the entire range of θ, and therefore, the amplitude of $\mathbf{E}\times\mathbf{B}$ velocity is constant. For simplicity, this degree of freedom (V_θ) in the velocity space will be omitted since it does not alter the results of our calculations.

[8] Equation (3) stipulates that for any $r\le r_s$, there exists a 1D Vlasov equation in the parallel direction, but these parallel Vlasov equations for different r are not independent. Instead, their mutual relation in the perpendicular direction is determined by the perpendicular profile of Φ. This is because Φ is a potential collectively produced by the plasma particles. Once Φ is determined from the boundary condition, it determines how the plasma distributes itself to self-consistently support the potential. Therefore, we only need to solve the equation for a particular r. Setting $r=\bar{r}$, a constant, define

$$\phi(z)=\Phi(\bar{r},z),$$
$$f(z,v)=F(\bar{r},z,v).$$

Now substitute the potential constructed in Equation (2) into Equation (1), replace r by $\bar{r}$, and re-write $\rho(\bar{r}, z)$ in terms of the rapped and passing electron distribution, f_{tr} and f_p, respectively. In terms of these variables, Equation (1) becomes

$$\frac{\partial^2\phi(z)}{\partial z^2}-k_\perp^2\phi(z)=\int_{-\phi}^{0}dw\frac{f_{tr(w)}}{2\sqrt{w+\phi}}+\int_{0}^{\infty}dw\frac{f_{p(w)}}{2\sqrt{w+\phi}}-1 \tag{4}$$

where $k_\perp=\frac{l_{00}}{r_s}\simeq\frac{2.404}{r_s}$, and $w=v^2-J_0(k_\perp\bar{r})\phi_{\|}(z)$ is the total energy of an electron at $\bar{r}$ traveling along z. Electrons with $w\ge 0$ are untrapped, and electrons with $w<0$ are trapped. Equation (4) differs from its counterpart in the 1D model by the term $k_\perp^2\phi$, which couples the perpendicular information of the solitary wave into its parallel equation. The larger the perpendicular size, r_s, the closer Equation (4) approaches its counterpart in the 1D model. In the limiting case when r_s approaches infinity, the solution reduces to the 1D solution that describes infinitely large charge sheets perpendicular to B and propagating along B. This is exactly the equivalent 3D system of the 1D model. The perpendicular size of the solitary wave determines whether a spacecraft would be able to see the 3D structure or only the parallel feature. This offers a plausible explanation as to why in the magnetosphere both multi and one dimensional solitary waves are seen. (See *Ergun et al.*, 1998 for multi-dimensional cases and see *Bale et al.*, 1998 and *Matsumoto et al.*, 1994 for 1D cases.)

[9] To obtain f_{tr}, we follow the BGK approach with Maxwellian ambient electrons,

$$F_p(W)=\frac{2}{\sqrt{\pi}}e^{-W}, \tag{5}$$

where $W=v^2-\Phi(r,z)$ is the total energy of an electron and is related to w by the relation $W(v,\bar{r},z)=w(v,z)$. For convenience, define $J_0(k_\perp\bar{r})\Psi$ as ψ. The trapped electron distribution obtained from Equation (4) then reduces to

$$f_{tr}(w)=-\frac{4k_\perp^2}{\pi}\sqrt{-w}+\frac{4\sqrt{-w}}{\pi\delta^2}\left[1-2\ln\left(\frac{-4w}{\psi}\right)\right]+\frac{2\exp(-w)}{\sqrt{\pi}}\left[1-\mathrm{erf}\left(\sqrt{-w}\right)\right]. \tag{6}$$

$f_{tr}(w)$ has to be non-negative for the solution to be physical and since $f_{tr}(0>w\ge-\psi)\ge f_{tr}(w=-\psi)$, the condition $f_{tr}(w=-\psi)\ge 0$ suffices to satisfy the requirement. From this condition, we obtain an inequality relation between δ, ψ and r_s,

$$\delta\ge\sqrt{\frac{4\ln 2-1}{\sqrt{\pi}e^{\psi}\left(1-\mathrm{erf}(\sqrt{\psi})/2\sqrt{\psi}-2.404^2/r_s^2\right.}}. \tag{7}$$

We do not restrict to EHs with zero phase space density at the center ($f_{tr}(w=-\psi)=0$) as did by *Muschietti et al.* [1999]. Therefore, for an allowed pair of (ψ, r_s), any δ that satisfies inequality (7) is allowed. In other words, for a fixed amplitude and perpendicular scale size, the parallel scale size has a lower bound but no upper bound. The lower bound corresponds to EHs with no trapped electrons at rest at the bottom of the potential energy troughs. The denominator on the right-hand side of inequality (7) has to be positive. This yields another inequality relation between ψ and r_s,

$$r_s>\frac{2.404}{\sqrt{\sqrt{\pi}e^{\psi}\left(1-\mathrm{erf}(\sqrt{\psi})/2\sqrt{\psi}\right.}}. \tag{8}$$

Equation (8) means that for a given potential amplitude, the perpendicular scale size of EHs is greater than a critical value given by the right-hand side in order to have a physical solution for the trapped electron distribution.

3. Illustration of Results

[10] Figures 1a–1c show plots of the allowed parameter range with Figure 1a representing equation (8), Figures 1bequation (7), and Figures 1cr_s cuts of equation (7). For a solitary potential Φ with a peak amplitude Ψ, the perpendicular size r_s has to satisfy equation (8) with the ψ on the right-hand side replaced by Ψ. For example, if Ψ is 0.5 (in units of T_e/e), the perpendicular size is roughly greater than 3 (in units of λ_D). We indicate the allowed region by O and the forbidden by X in Figures 1a and 1b. Any (δ, Ψ, r_s) lying on or above the shaded surface is allowed. For example, for Ψ = 100 (corresponding to 10 kV for T_e = 100 eV) and r_s = 100 (corresponding to 10 km for λ_D = 100 m), the parallel scale size δ can be as small as 20 (λ_D) and as large as several earth radii (R_E) or even larger. The inequality nature of the width-amplitude-perpendicular size relation implies that the plasma permits large scale BGK EHs with reasonable amplitudes. Figure 1c shows the dependence of the parallel width-amplitude (δ-ψ) relation on the perpendicular size r_s. With a fixed r_s, the empty-centered EHs (corresponding to the equal sign in equation (7)) give the largest amplitudes for the same δ. For the same amplitude, EHs with larger r_s have smaller lower bounds for δ.

[11] Figure 1d plots an example of the solitary potential Ψ as a function of r and z with r_s = 5, Ψ = 0.5, and δ = 2, in the allowed parameter range. The Φ with the above parameter set is used to derive the structures of the electric field and charge density. As the solitary waves travel fast along B with typical velocity ~1000 km/s

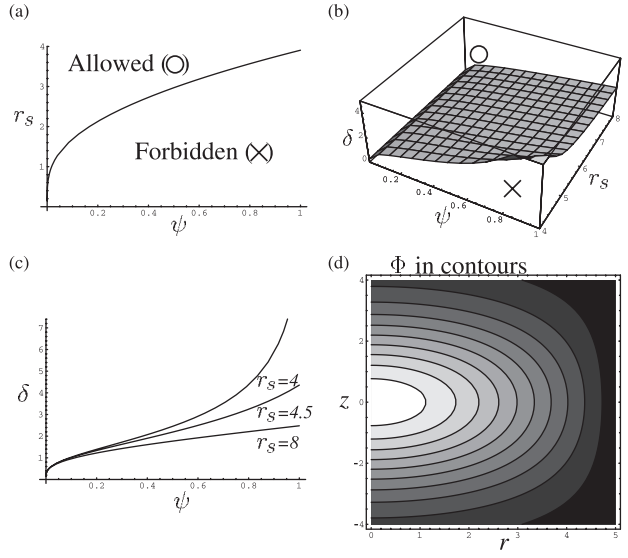

Figure 1. The inequality relation between the perpendicular size (r_s) and the potential amplitude (ψ) in (a); the inequality relation between the perpendicular size, parallel size (δ) and the amplitude in (b); three r_s cuts showing the dependence of the parallel width (δ)-amplitude (ψ) relation on the perpendicular size in (c); a sample solitary potential as a function of z and r in (d). Solitary potentials can take (r_s, δ, ψ) values in regions marked Allowed (O). Regions marked Forbidden (X) give unphysical trapped electron distributions and are thus not allowed.

and pass the spacecraft, the measurement taken on the spacecraft is analogous to taking parallel cuts of the involved quantities. We will plot the parallel cuts for comparison with the observations. The electric field of the solitary structure vanishes at the center and

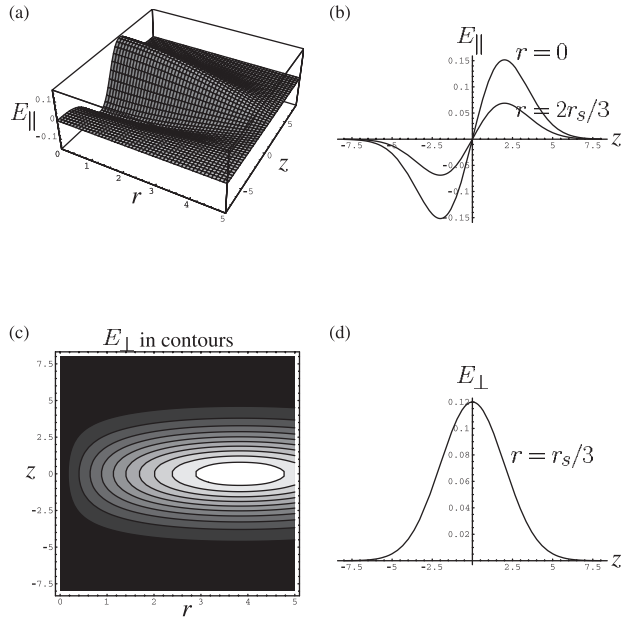

Figure 2. (a) and (c): The parallel and perpendicular components of the electric field for the constructed BGK solitary wave. $E_\parallel$ is symmetric bipolar along z and falls off to zero as J_0 along r. $E_\perp$ is unipolar along z and it rises and falls as J_1 along r. (b): Two parallel cuts of $E_\parallel$ along the symmetry axis ($r = 0$) and along $r = 2r_s/3$ showing that they are bipolar pulses. (d): A parallel cut of $E_\perp$ along $r = 2r_s/3$. It is unipolar just as observed in space observations.

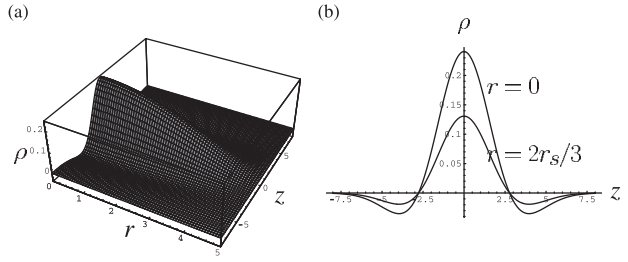

Figure 3. (a): The charge density for the constructed BGK solitary wave. In the parallel direction (z), it is positive at the core and negative at the flank. Along the perpendicular direction (r), the positive and negative excursions decrease monotonically to zero as r increases to r_s. (b): Two parallel cuts of the charge density along the symmetry axis ($r = 0$) of the solitary wave and along $r = 2r_s/3$ showing the excursions in fractions of the ambient plasma density.

points outward. The parallel component of the electric field, $E_z \equiv E_\parallel$, is shown in Figure 2a as a function of r and z. On the symmetry axis, $r = 0$, the maximum excursion of $E_\parallel$ is the largest and as r increases, it falls off as $J_0(k_\perp r)$. Two parallel cuts of $E_\parallel$ at $r = 0$ and $r = r_s/1.5$ are shown in Figure 2b. For any $\bar{r} < r_z$, $E_\parallel(\bar{r}, z)$ is symmetric and bipolar. The perpendicular component of the electric field, $E_r \equiv E_\perp$, is plotted in Figure 2c as a contour plot to aid in the visualization for its parallel cuts. The perpendicular profile of $E_\perp$ is $J_1(k_\perp r)$. One example of the parallel cuts is shown in Figure 2d and it is unipolar. Any parallel cut of $E_\perp$ is unipolar except the one along the symmetry axis ($r = 0$) where $E_\perp$ is zero. Note that $E_\perp$ is not zero at the perpendicular boundary, $r = r_s$, so perpendicular screening from the ambient electrons is needed to facilitate the decrease of $E_\perp$ to zero. This additional screening is not described by our solution.

[12] The charge distribution ρ as a function of r and z is presented in Figure 3a, and two parallel cuts of ρ are depicted in Figure 3b. Note as the radial distance from the symmetry axis increases, the the measured charge density perturbation becomes smaller. Along the symmetry axis, the charge density variation is the largest with the positive excursion reaching ~24%, and the negative ~4%. An off-centered cut along $r = r_s/1.5$ with a positive excursion ~13% and ~2% negative is also shown.

4. Summary and Conclusion

[13] In summary, analytical solutions for BGK electron solitary waves have been constructed incorporating the 3D electrical interaction of plasma. Pictorially, the solution is like a perpendicularly confined bundle of BGK EHs (1D). This solution retains the features of the 1D BGK model [*Muschietti et al.*, 1999], and qualitatively reproduces the observed bipolar $E_\parallel$ and unipolar $E_\perp$. If the perpendicular size $r_s \to \infty$, the solution reduces to the 1D BGK solution.

[14] In addition to what one learns from the 1D BGK model [*Muschietti et al.*, 1999], our solutions provide several pieces of new information: 1. The width-amplitude relation is an inequality which permits the possibility of having large scale EHs with reasonable potential amplitudes. Large scale EHs could be a macroscopic feature of the magnetosphere and can play important roles in particle energization processes. 2. The parallel width-amplitude relation depends on the perpendicular size. This dependence can be used in conjunction with the measured parallel width-amplitude (unbinned) scatter plot to yield an estimate of the typical perpendicular size of EHs. 3. The electric field of our constructed EHs is radially outward and an ensemble of EHs can heat the ions efficiently in the perpendicular direction [*Ergun et al.*, 1999].

[15] **Acknowledgments.** Research at the Universities of Washington and California at Berkeley is funded in part by NASA grants NAG5-3170 and NAG5-26580.

References

Bale, S. D., et al., Bipolar electrostatic structures in the shock transition region: Evidence of electron phase space holes, *Geophys. Res. Lett.*, *25*, 2929, 1998.

Bernstein, I. B., J. M. Greene, and M. D. Kruskal, Exact nonlinear plasma oscillations, *Phys. Rev.*, *108*, 546, 1957.

Boström, R., Characteristics of solitary waves and double layers in the magnetospheric plasma, *Phys. Rev. Lett.*, *61*, 82, 1988.

Cattell, C. A., et al., Comparisons of Polar satellite observations of solitary wave velocities in the plasma sheet boundary and the high altitude cusp to those in the auroral zone, *Geophys. Res. Lett.*, *26*, 425, 1999.

Chen, L.-J., and G. K. Parks, Trapped and passing electrons in BGK solitary waves, physics/0103020, 2001.

Ergun, R. E., et al., FAST satellite observations of large-amplitude solitary structures, *Phys. Rev. Lett.*, *25*, 2041, 1998a.

Ergun, R. E., et al., Debye-scale plasma structures associated with magnetic-field-aligned electric fields, *Phys. Rev. Lett.*, *81*, 826, 1998b.

Ergun, R. E., et al., Properties of fast solitary structures, *Nonlinear Processes in Geophys.*, *6*, 187, 1999.

Franz, J., et al., POLAR observations of coherent electric field structures, *Geophys. Res. Lett.*, *25*, 1277, 1998.

Kojima, H., et al., Geotail wave form observations of broadband/narrowband electrostatic noise in the distant tail, *J. Geophys. Res.*, *102*, 14,439, 1997.

Matsumoto, H., et al., Electrostatic solitary waves (ESW) in the magnetotail: BEN wave forms observed by Geotail, *Geophys. Res. Lett.*, *21*, 2915, 1994.

Mozer, F. S., et al., New features of time domain electric-field structures in the auroral acceleration region, *Phys. Rev. Lett.*, *79*, 1281, 1997.

Muschietti, L., et al., Phase-space electron holes along magnetic field lines, *Geophys. Res. Lett.*, *26*, 1093, 1999.

Mälkki, A., et al., On theories attempting to explain observations of solitary waves and weak double layers in the auroral magnetosphere, *Phys. Scr.*, *39*, 787, 1989.

Temerin, M., et al., Observations of double layers and solitary waves in the auroral plasma, *Phys. Rev. Lett.*, *48*, 1175, 1982.

Li-Jen Chen, Physics Department, University of Washington, Seattle, WA 98195, USA. (lijen@u.washington.edu)

George K. Parks, Space Sciences Laboratory, University of California, Berkeley, CA 94720, USA.